

Infrared active surface modes found in thin films of perfluoroalkanes reveal the dipole-dipole interaction and surface morphology

Cite as: J. Chem. Phys. **153**, 044703 (2020); <https://doi.org/10.1063/5.0012910>

Submitted: 06 May 2020 . Accepted: 29 June 2020 . Published Online: 22 July 2020

Aki Fukumi, Takafumi Shimoaka , Nobutaka Shioya , Naoto Nagai , and Takeshi Hasegawa 



View Online



Export Citation



CrossMark

ARTICLES YOU MAY BE INTERESTED IN

[Morphology-sensitive infrared absorption bands of polymers derived from surface polaritons](#)

AIP Advances **9**, 105203 (2019); <https://doi.org/10.1063/1.5116280>

[Ultrathin porphyrin and tetra-indole covalent organic frameworks for organic electronics applications](#)

The Journal of Chemical Physics **153**, 044702 (2020); <https://doi.org/10.1063/5.0010164>

[N₃⁺: Full-dimensional ground state potential energy surface, vibrational energy levels, and dynamics](#)

The Journal of Chemical Physics **153**, 044302 (2020); <https://doi.org/10.1063/5.0011957>

Lock-in Amplifiers
up to 600 MHz



Infrared active surface modes found in thin films of perfluoroalkanes reveal the dipole–dipole interaction and surface morphology

Cite as: *J. Chem. Phys.* **153**, 044703 (2020); doi: [10.1063/5.0012910](https://doi.org/10.1063/5.0012910)

Submitted: 6 May 2020 • Accepted: 29 June 2020 •

Published Online: 22 July 2020



Aki Fukumi,¹ Takafumi Shimoaka,¹  Nobutaka Shioya,¹  Naoto Nagai,²  and Takeshi Hasegawa^{1,a)} 

AFFILIATIONS

¹Laboratory of Chemistry for Functionalized Surfaces, Division of Environmental Chemistry, Institute for Chemical Research, Kyoto University, Gokasho Uji, Kyoto 611-0011, Japan

²Industrial Research Institute of Niigata Prefecture, 1-11-1 Abumi Nishi, Niigata 950-0915, Japan

^{a)}Author to whom correspondence should be addressed: htakeshi@scl.kyoto-u.ac.jp

ABSTRACT

Infrared (IR) spectra of an organic thin film are mostly understood by considering the normal modes of a single molecule, if the dipole–dipole (D–D) interaction is ignorable in the film. When the molecules have a chemical group having a large permanent dipole moment such as the C=O and C–F groups, the D–D interaction induces vibrational couplings across the molecules, which produces an extra band as a surface phonon or polariton band because of the small thickness. Since the dipole moment of an organic compound is much less than that of an inorganic ionic crystal, we have a problem that the extra band looks like a normal-mode band, which are difficult to be discriminated from each other. In fact, this visual similarity sometimes leads us to a wrong direction in chemical discussion because the direction of the transition moment of the extra band is totally different from those of the normal modes. Here, we show useful selection rules for discussing IR spectra of a thin film without performing the permittivity analysis. The apparent change in the spectral shape on decrease in the thickness of the sample can be correlated with the morphological change in the film surface, which can also be discussed with changes in the molecular packing. This analytical technique has effectively been applied for studying the chemical properties of perfluoroalkanes as a chemical demonstration, which readily supports the stratified dipole-array theory for perfluoroalkyl compounds.

Published under license by AIP Publishing. <https://doi.org/10.1063/5.0012910>

INTRODUCTION

Perfluoroalkyl (R_f) compounds are attracting increased interest in recent years from the view point of physical chemistry^{1,2} involving surface chemistry^{3–5} and surface spectroscopy,^{6,7} since understanding of material properties of a single molecule is being rapidly progressed in a separated manner from that of macroscopic properties in a lucid theoretical framework in the stratified dipole-array (SDA) theory.^{1,2} Various experiments on surface chemistry and spectroscopy have already confirmed that R_f compounds are intrinsically different from hydrocarbons. The most prominent characteristic of R_f compounds is that the molecules are spontaneously aggregated by the dipole–dipole (D–D) interactive force (i.e., orientation effect), whereas hydrocarbon molecules are aggregated by London's dispersion force.^{8,9} On a macroscopic scale, the dipole

moment of each C–F bond becomes nearly invisible because of the summation of the dipole arrays having various directions,² which accounts for the various R_f -specific material properties of aggregated molecules as represented by the dielectric, fluorous, and other chemical properties.

R_f compounds have unique characters not only in material properties but also in vibrational spectra. Since the mass of fluorine is larger than that of carbon, the dispersion relation between the angular frequency and the wavenumber is largely different from that of hydrocarbons, which results in a huge discrepancy between the infrared (IR) and Raman band positions. For example, the band of the symmetric CF_2 stretching vibration [$\nu_s(CF_2)$] mode appears at $\sim 1150\text{ cm}^{-1}$ in IR spectra, whereas it appears at $\sim 720\text{ cm}^{-1}$ in Raman spectra.^{10,11} R_f compounds also exhibit a unique higher-wavenumber shift of the $\nu_s(CF_2)$ band with an increase in the R_f

chain length, whereas hydrocarbons exhibit a lower-wavenumber shift.¹¹ In addition, R_f molecules are spontaneously aggregated because of the helical conformation cooperated with the D–D interaction, and therefore, the aggregate exhibits chirality, which can be detected by Raman optical activity,¹² which never happens in a normal hydrocarbon.

Furthermore, R_f compounds are known to give an “extra band” that has a very similar shape and intensity to those of the normal-mode bands, since the C–F bond has a fairly large permanent dipole moment.^{13,14} Since the discrimination of the extra band from normal absorption bands is fairly difficult, the extra band is often misunderstood as a normal-mode band inappropriately, which leads the chemical discussion in a wrong direction. The origin of the extra band is attributed to a coupled oscillation of a molecular aggregate via the D–D interaction.¹⁴ If the D–D interaction is strong enough to be coupled with IR light, the polariton is the origin of the extra band, which yields negative permittivity.^{15–17} Thus far, therefore, the analysis of electric permittivity has long been a key technique to find the polariton band.^{13,14}

In the present study, we have found that the extra band of an organic thin film buried in normal-mode bands can be identified by a simple IR attenuated total-reflection (ATR) technique without performing the permittivity analysis, which can further be attributed to the surface modes¹⁸ of a slab or particle phonon/polariton. This study is performed on a series of “ n -perfluoroalkanes” with different lengths varying from C_6F_{14} to C_9F_{20} that are all liquid at ambient temperature. During the evaporation of the liquid, the IR ATR spectra changed significantly not only in the intensity but also in the shape especially for a very thin film remaining on the ATR prism. The shape change is not induced by a chemical interaction but by the extra band due to the surface mode of a molecular aggregate as a result of the D–D interaction.

In addition, on appearance of the thin-film specific extra band, another important key band, which is the symmetric CF_2 stretching vibration band, exhibits an apparent higher-wavenumber shift. This simultaneous change in the two key bands implies that molecular aggregation has largely been lost on thinning of the film. This apparent shift was found for a series of compounds of C_6F_{14} – C_8F_{18} , but C_9F_{20} did not show the shift at all. This boundary beautifully corresponds to the critical length of R_f -containing compounds revealed by the SDA theory. In this manner, the surface modes are found quite useful for discussing IR spectra of organic thin films as well as the normal modes.

EXPERIMENTAL SECTION

Sample preparation

A series of perfluoroalkanes having different chain lengths were obtained as follows. Perfluorohexane (C_6F_{14}) with a purity of 95%, perfluorooctane (C_8F_{18}) with a purity of 98%, and perfluorononane (C_9F_{20}) with a purity of 97% were purchased from Sigma-Aldrich Co. LLC (St. Louis, MO, USA). Perfluoroheptane (C_7F_{16}) with a purity of 98% was purchased from PCR Research Chemicals, Inc. (Gainesville, FL, USA). The impurity is assigned to perfluoropentane (C_5F_{12}) by the providers. Since the bp of the samples was in good agreement with reference data, they were used without further purification.

IR ATR measurements

The evaporation process of a perfluoroalkane was monitored by measuring IR ATR spectra with a PIKE Technologies (Madison, WI, USA) VeeMax[®] III ATR attachment having an ATR prism of germanium (Ge). The angle of incidence was fixed at 45° , and un-polarized light was used unless otherwise stated. For the s-polarization measurements, a Jasco (Tokyo, Japan) gold wire-grid linear polarizer built on zinc selenide was used. After putting a droplet sample with a volume of $\sim 30 \mu\text{L}$ on the ATR prism, the IR ATR measurements were performed on a Thermo Fisher Scientific (Madison, WI, USA) Nicolet 6700 FT-IR spectrometer having a mercury cadmium telluride (MCT) detector with the rapid-scan mode measured every one second during evaporation. No accumulation was carried out for each measurement, and the wavenumber resolution was 8 cm^{-1} to keep the signal-to-noise ratio (SNR) good enough. The peak position was read not at the apparent peak top but at the center position of the band. All the measurements were performed under ambient pressure and temperature.

RESULTS AND DISCUSSION

Thin-film specific spectrum appeared on evaporation

Figure 1 presents IR ATR spectra of C_6F_{14} on evaporation with time measured on the ATR prism of Ge. The sample is prepared by putting a droplet of liquid on the prism at ambient temperature (bp 60°C), and the thickness at the initial stage is $\sim 1 \text{ mm}$, which is much larger than the penetration depth of the ATR measurement ($\sim 1 \mu\text{m}$). In the initial spectrum marked by red, the bands at 1205 cm^{-1} and

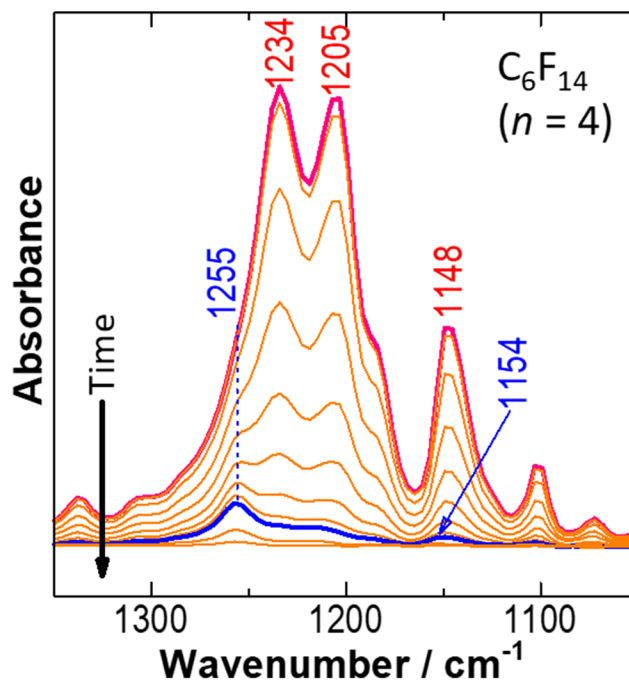


FIG. 1. Selected time-dependent IR ATR spectra of C_6F_{14} deposited on Ge during the evaporation process at ambient temperature.

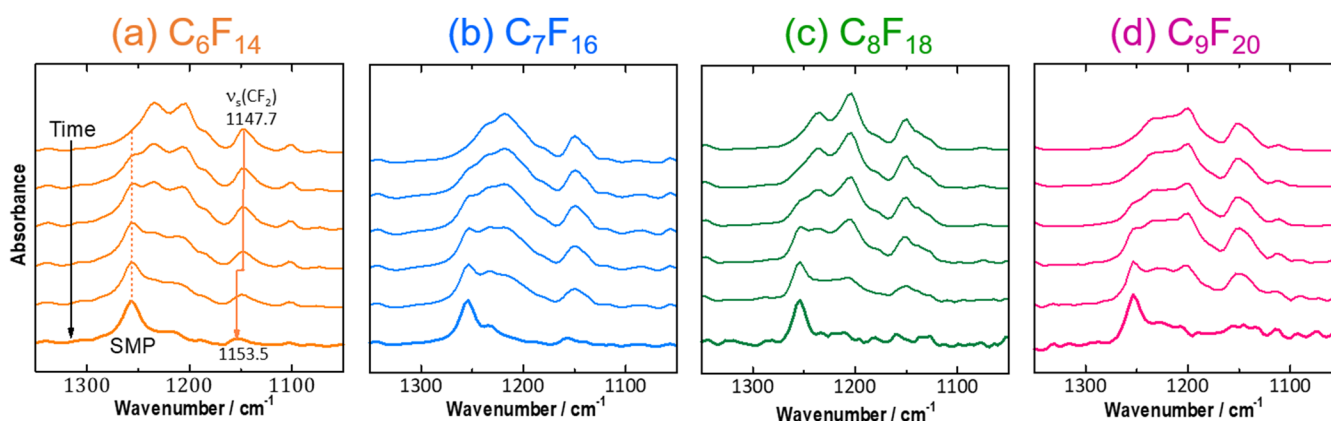


FIG. 2. IR ATR spectra of the evaporation process of perfluoroalkanes with different chain lengths.

1148 cm^{-1} have already been confirmed to be the chain stretching vibration and the symmetric CF_2 stretching vibration ($\nu_s\text{CF}_2$) band, respectively,^{10,11} whereas the assignment of the most intensive band at 1234 cm^{-1} has long been under discussion. This unconfirmed band is sometimes temporarily assigned to the anti-symmetric CF_2 stretching vibration [$\nu_a(\text{CF}_2)$] band, but this assignment should be very inaccurate because it yields an inconsistent result with those using other established bands especially when molecular orientation analysis is performed in a thin film.¹⁹ In this sense, this band is a matter to be revealed in the present study.

Since the number of CF_2 groups of the compound ($n = 4$) is less than the critical length of the SDA spontaneous molecular packing ($n = 7$),^{1,2} the molecular aggregation is relatively weak accounting for the quick evaporation. In fact, the sample visually disappeared in only 10 s. Of surprise is that the spectral shape significantly changes at the last stage of the spectral measurements as represented by the blue curve. Thanks to the fairly large permanent dipole moment of the C–F bond,⁸ even the very thin layer remaining at the last moment still exhibits a good spectrum with a high SNR for our quantitative analysis. The great change is represented by disappearance of the prominent band at 1234 cm^{-1} , and instead, a new band at 1255 cm^{-1} develops. The shift of 21 cm^{-1} is too large, however, to attribute the changes to the molecular aggregation or related things on considering that the $\nu_s(\text{CF}_2)$ band is known to exhibit a very minute change in aggregation or crystallization.^{4,20}

On closer inspection, the new band is also found on a shoulder of the intermediate spectra, which makes an impression on us that it may be related to the molecules that are directly interacting with the substrate surface. The same shape change was, however, reproduced on other materials (data not shown). Therefore, the blue spectrum is not induced by the interaction with the substrate surface, either. In other words, the shape of the blue spectrum should have a strong correlation with the thickness of the thin film surface.

When the same experiments are performed for other compounds having different chain lengths, a very similar spectral change is reproduced, as shown in Fig. 2. The commonly found results straightforwardly imply that the spectral change in shape should simply be attributed to the “thinning” of the film. Another possibility is a change in molecular arrangement in the thin film involving

the orientation change. The shape change is, however, too significant to be explained by the molecular packing, conformation, and orientation.²⁰ In addition, as shown later, the spectral change is found irrespective of polarizations. Therefore, another idea should be employed for explanation of the shape change, that is, a physical reason that considers not only the normal mode of a molecule but also a coupled oscillation over the molecular aggregate in the film.

Surface modes in a thin film

The thin-film specific spectral shape reminds us of the surface mode that is found as Berreman's mode¹⁵ of phonon and of surface polariton (SP). To put the basic concept of phonon and polariton in our mind, let us imagine ionic crystals represented by sodium chloride for simplicity. In the crystal, an ionic pair of Na^+ and Cl^- has a large dipole moment (9.00 D),²¹ and the dipole vibration propagates through the crystal via the D–D interaction three-dimensionally for a long distance. As a result, the crystal has a coupled oscillation of the lattice of dipoles, that is, the phonon.¹⁵ Optical properties of phonons can readily be theorized by using the frequency-domain electric permittivity $\epsilon(\omega) = \epsilon_0\epsilon_r(\omega)$, where^{6,7,15}

$$\epsilon_r(\omega) = \epsilon_{r,\infty} + \frac{(\epsilon_{r,0} - \epsilon_{r,\infty})\omega_{\text{TO}}^2}{\omega_{\text{TO}}^2 - \omega^2 - i\gamma\omega}. \quad (1)$$

Here, ϵ_0 and ϵ_r are the vacuum and relative permittivity, respectively. $\epsilon_{r,0}$ and $\epsilon_{r,\infty}$ are the static and high-frequency relative permittivity, respectively. ω_{TO} is the angular frequency of the harmonic transverse-optic (TO) bulk phonon of the crystal, and ω is the angular frequency of the IR light for the observation. γ is the damping factor, which determines the propagation distance in the crystal. For a long-distance propagation of vibration as found in an inorganic ionic crystal, γ can be set to zero. In this approximation, Eq. (1) is largely simplified to have the real part only [Eq. (2)],^{6,15,16}

$$\epsilon_r(\omega) = \epsilon_{r,\infty} + \frac{(\epsilon_{r,0} - \epsilon_{r,\infty})\omega_{\text{TO}}^2}{\omega_{\text{TO}}^2 - \omega^2}. \quad (2)$$

The angular frequency of the longitudinal-optic (LO) phonon is correlated with that of the TO one by the Lyddane–Sachs–Teller equation²²

$$\omega_{\text{LO}}^2 = \frac{\epsilon_{r,0}}{\epsilon_{r,\infty}} \omega_{\text{TO}}^2. \quad (3)$$

On considering both equations (2) and (3), ϵ_r becomes nil at $\omega = \omega_{\text{LO}}$, which leads to $\nabla \times \mathbf{E} = 0$ accounting for the longitudinal wave.⁶

The oscillator strength corresponding to $\epsilon_{r,0} - \epsilon_{r,\infty}$ ⁶ is fairly large for ionic crystals, which results in apparent negative permittivity for a large part between ω_{TO} and ω_{LO} (yellow zone in Fig. 3). The negative permittivity generates a pure imaginary wavenumber on considering the dispersion relation of $c^2 k^2 = \omega^2 \epsilon_r(\omega)$, which yields an extraordinarily high reflectance (or extremely low transmittance) in the wavenumber region, which is known as the Reststrahlen band.¹⁶ In short, the high reflectance is strongly correlated with the negative permittivity, both of which are a useful marker of existence of phonon.¹⁴ As a matter of fact, ionic crystals typically exhibit a huge LO–TO splitting $[(\omega_{\text{LO}} - \omega_{\text{TO}})/2\pi c]$ of more than 100 cm^{-1} .

In the case of an organic compound, however, the situation greatly changes. Organic compounds mostly have a much weaker IR absorption, and the molecular order is less (sometimes in amorphous) than that in inorganic ionic crystals.^{13,14} As a result, even a strong IR absorber having the carbonyl group²¹ exhibits a much smaller LO–TO shift of $\sim 10 \text{ cm}^{-1}$ at most.²⁴ As a result, the corresponding permittivity dispersion also becomes minor, and the lowest permittivity remains positive except in some strong IR absorbing polymeric materials.¹⁴ In this case, the damping factor cannot be nil because the vibration propagation via the D–D interaction is limited, and Eq. (1) must be taken into account. A schematic permittivity of such a strong IR absorbing organic material is presented in Fig. 4(a), in which two constituents (marked by the two red marks) of the imaginary part (pink curve) are partly overlapped resulting in a very sharp drop-down of the real part, but the bottom of the real

part remains positive. By using this permittivity, a normal-incidence transmission spectrum is calculated by using the following equation⁷ as presented by the black curve in Fig. 4(b):

$$A = \frac{4d_2\omega}{\ln 10 \cdot c} \cdot \frac{1}{1 + n_3} \text{Im}(\epsilon_{r,2}). \quad (4)$$

Here, the parameters c , d_2 , and n_3 are the light velocity, thickness of the film, and refractive index of the substrate, respectively. Details of the parameters for the calculation are available in the caption of Fig. 4. The simulated black spectrum is nearly the same as the TO function (red curve) having no influence of the LO curve (blue).

When the sample is tilted at 45° and subjected to p -polarization, on the other hand, a new band appears as a shoulder on the higher-wavenumber side [Fig. 4(c)], which corresponds to the LO function. This is the Berreman phonon band that should strictly be discriminated from a normal-mode band of a molecule. In our actual case, the C–F bond has a large permanent dipole moment, and the bands at 1234 cm^{-1} and 1205 cm^{-1} are close to each other, which is the same as in the simulation in Fig. 4. Therefore, a new band at 1255 cm^{-1} in Fig. 1 is expected on the higher-wavenumber side as the Berreman mode. In this manner, the band at 1255 cm^{-1} is temporally assigned to the Berreman mode that is similar to the bulk LO mode.^{6,16,17}

Surface-polariton mode

Berreman's effect has an intuitive image that a nearly collective vibration of the molecules induces the surface charges on both surfaces of the flat thin film, and a surface-perpendicular polarity appears between the surface charges, which can be detected by only p -polarization at an oblique angle of incidence particularly by the reflection–absorption technique.^{3,7,25} If the largely shifted band at 1255 cm^{-1} is truly attributed to the Berreman effect, we thus receive an impression that the film at the last moment of evaporation remains as a continuous flat film on the ATR prism surface.

To consider surface modes, we also have to take the surface polariton (SP)¹⁵ into account. The SP is an alternative mode of phonon when it is strongly coupled with the IR light. The strong coupling attains a different quantum state from phonon: not only the incident IR light but also the emitted light from the phonon is re-absorbed by the phonon, which requires a concept of time-retardation.^{6,13–17} To theorize the SP mode, therefore, all the Maxwell equations and the constituent equations must fully be employed.^{6,16,17,26} For a flat surface of a slab, the SP mode appears between the TO and LO angular frequencies,^{16,17} but this non-radiative mode on a slab can be observed by using the surface electromagnetic wave (SEW) technique.¹⁵ This mode, therefore, should strictly be discriminated from the Berreman mode technically. In this article, the SP mode on a flat film can be excluded because the SEW technique is not used.

Another notable case of the SP is found on materials having a surface morphology like particles. Particularly when the particle size is $\sim 1 \mu\text{m}$ or larger for IR spectroscopy, the time-retardation specific to polaritons cannot be ignored,¹⁷ and a radiative mode of SP appears in the IR spectra because the radiative mode can readily be coupled with the incident light without a special technique such as the SEW. If the particle size is small, the time-retardation can be ignored (electrostatic approximation),^{17,27} and many surface

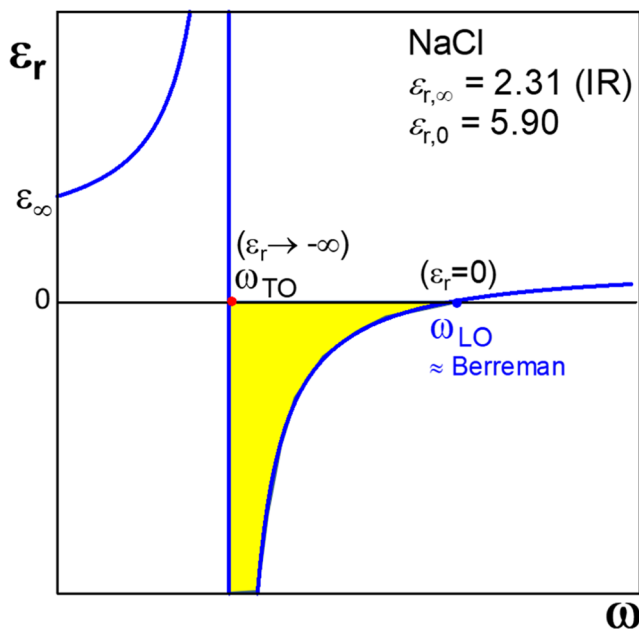


FIG. 3. Electric permittivity from Eq. (2) with $\epsilon_{r,\infty} = 2.31$, $\epsilon_{r,0} = 5.90$ ²³ for the sodium chloride crystal.

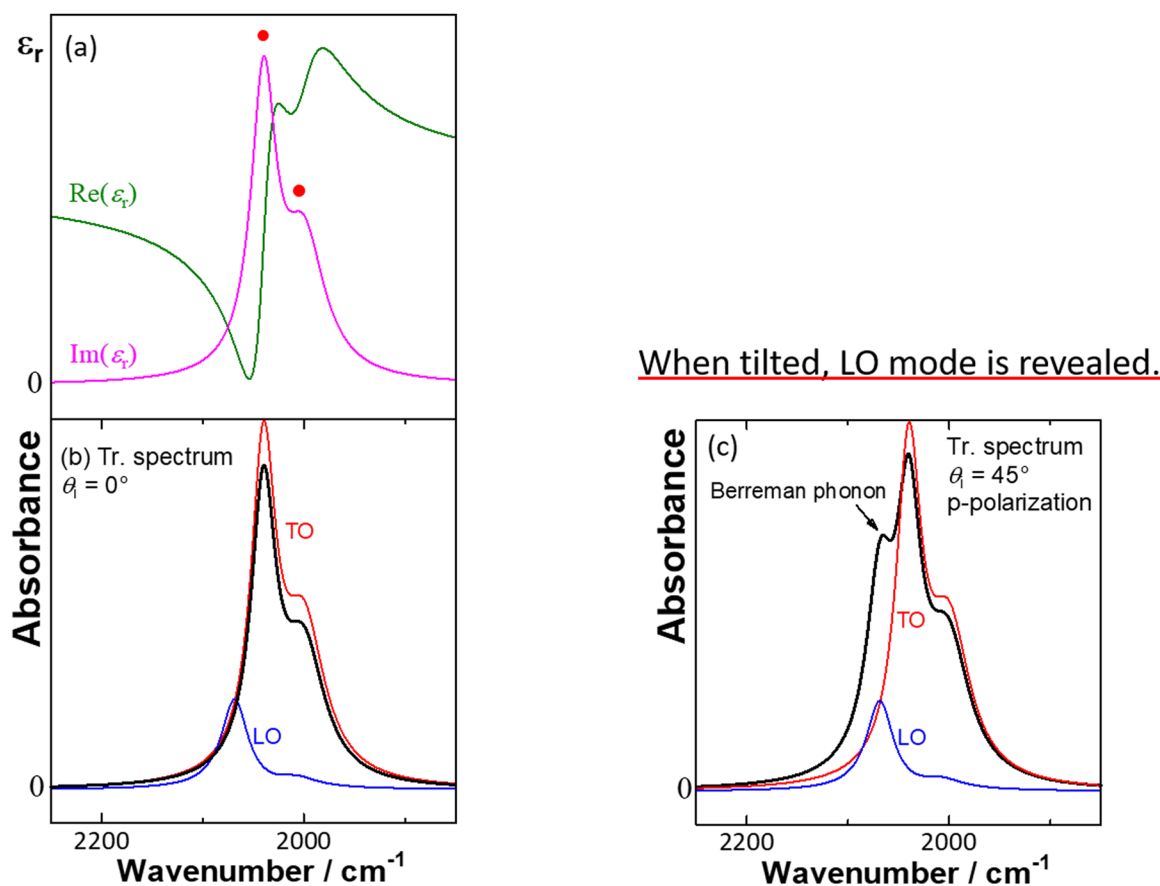


FIG. 4. Berreman mode of a flat thin film with a thickness of 2.5 nm on Ge ($n_3 = 4.0$) revealed by p -polarization. (a) Model permittivity function comprising two constituents marked by the two red marks, (b) a simulated IR transmission spectrum with normal incidence (black) with the TO and LO functions, and (c) a simulated IR transmission spectrum with an oblique incidence of 45° .

modes appear including the Fröhlich mode.²⁸ Since the retardation is ignored for solving Maxwell equations for the small particles, these modes have a similar background to that of phonons. Nevertheless, in both retardation and non-retardation cases, the “surface charges of particles” are a common schematic to exhibit the surface modes. In this sense, therefore, both modes can be categorized into a common “surface mode of particles (SMP).” An important common characteristic of the SMP is that the peak position is apparently smaller than that of the bulk LO mode,^{6,16,17} and it is observable by IR measurements irrespective of polarization.

Here, the characteristics of the thin-film specific spectra of a strong IR absorbing compound described above are summarized as the following two selection rules:

1. Berreman’s mode of a continuous flat film yields a similar spectrum to that of the bulk LO mode, and the peak position is also quite similar to that of the LO mode. The Berreman-mode spectrum, however, can be observed by p -polarization only with an oblique angle of incidence.
2. A discontinuous film having surface morphologies would yield the SMP bands, which have a similar shape to that of the bulk LO mode, but the peak position is apparently lower than that of the LO mode, which can be observed by both p -polarization and s -polarization.

To compare the spectral shapes, the red and blue spectra of Fig. 1 are re-plotted in Fig. 5(a). By the use of the ATR spectrum of the thick sample, the bulk LO and TO energy-loss functions are calculated, as presented in Fig. 5(b). The calculation was performed by the use of Plaskett and Schatz’s method²⁹ to obtain the complex permittivity, ϵ_r , which was used to have the LO [$\text{Im}(-1/\epsilon_r)$] and TO [$\text{Im}(\epsilon_r)$] functions. As expected, the calculated LO function readily reproduces the shape of the observed blue ATR spectrum of the thin film in Fig. 5(a). At this moment, the “shape” of the observed LO-like spectrum satisfies both selection rules.

To examine the peak positions, however, the observed spectrum of the thin film can be assigned to one of the rules: the TO

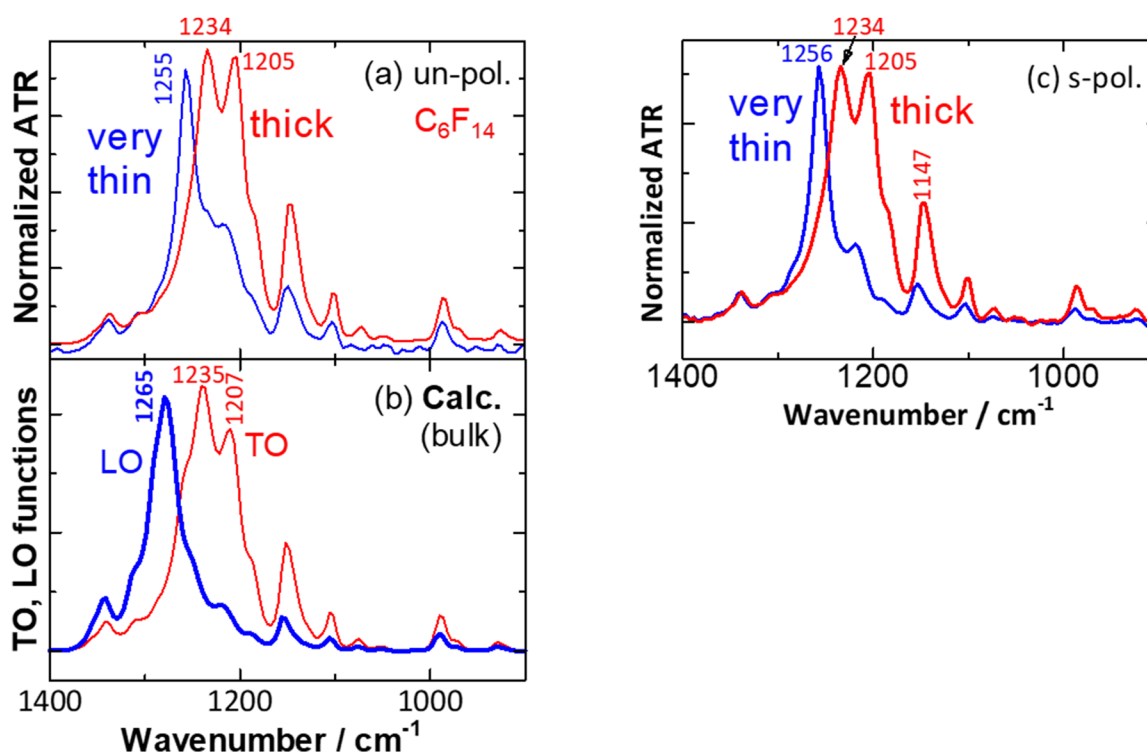


FIG. 5. Comparison of (a) the observed ATR spectra of C_6F_{14} with (b) the calculated bulk TO and LO functions. (c) The s -polarization spectra reproduce the un-polarized spectra.

function agrees fairly well with the thick-sample spectrum, whereas the thin-film spectrum exhibits an apparently lower wavenumber than that of the LO function by 10 cm^{-1} . This apparent shift suggests that the rule No. 2 should be appropriate for the spectral change. If this is true, then the s -polarization measurements should regenerate the spectral changes. In fact, as presented in Fig. 5(c), very similar results to that of Fig. 5(a) are obtained by the s -polarization measurement, too. Since Berreman's mode can be observed by p -polarization only, this result strongly supports the SMP model, that is, a discontinuous morphology of the film remained on the ATR prism surface. This reminds us of an experimental fact that a continuous monolayer film of an R_f compound prepared by the Langmuir–Blodgett technique does not show a spectrum having the LO function in shape.¹⁹

SDA molecular packing

With an appearance of the SMP peak in Fig. 2(a), on closer inspection, a very apparent peak shift is recognized for the $\nu_s(\text{CF}_2)$ band from 1147.7 cm^{-1} to 1153.5 cm^{-1} . This band is known to be a useful marker to discuss the molecular packing.^{1,2,4,7,19} When the packing becomes loose, the peak position moves to a higher wavenumber.

At the initial stage of the ATR measurements, the sample is a thick liquid layer, in which the R_f molecules are mostly surrounded by other R_f molecules: most of the molecules interact with each other

by a D–D interaction. When the sample is evaporated to be very thin, the film becomes discontinuous as revealed by the appearance of the SMP peak, in which the molecular aggregates have much “surfaces” having a smaller number of D–D interactions than the bulk sample. Therefore, the high-wavenumber shift occurs simultaneously with the appearance of the SMP peak, which is typically found in Fig. 6(a). A similar thing happens for the compounds C_7F_{16} and C_8F_{18} [Figs. 6(b) and 6(c)].

Nevertheless, the compound C_9F_{20} does not exhibit the shift even after the appearance of the SMP peak [Fig. 6(d)]. This difference can be understood by considering the SDA theory.² According to the theory, the spontaneous molecular interaction of R_f compounds is induced by the D–D interaction and the helical conformation cooperatively. As a result, R_f groups are known to be aggregated two-dimensionally, if the chain length, n , of the R_f group is “seven” or longer where the length is defined by the number of CF_2 groups. In our case, C_9F_{20} corresponds to $n = 7$, which is the critical length to induce the spontaneous aggregation. Therefore, an ordered packing of the C_9F_{20} molecules is expected even at the initial stage. Since the sample is liquid, nevertheless, both locally ordered and un-ordered aggregates should coexist in the liquid. As found in Fig. 6(d), even at 300 s (60 s later than the appearance of the SMP peak), no apparent “peak shift” is found, and instead, the plotted points are scattered because of a poor SNR of the very weak spectra. Even after the evaporation of most of the molecules, some molecular aggregates should be left on the ATR prism, in which the ordered molecular clusters

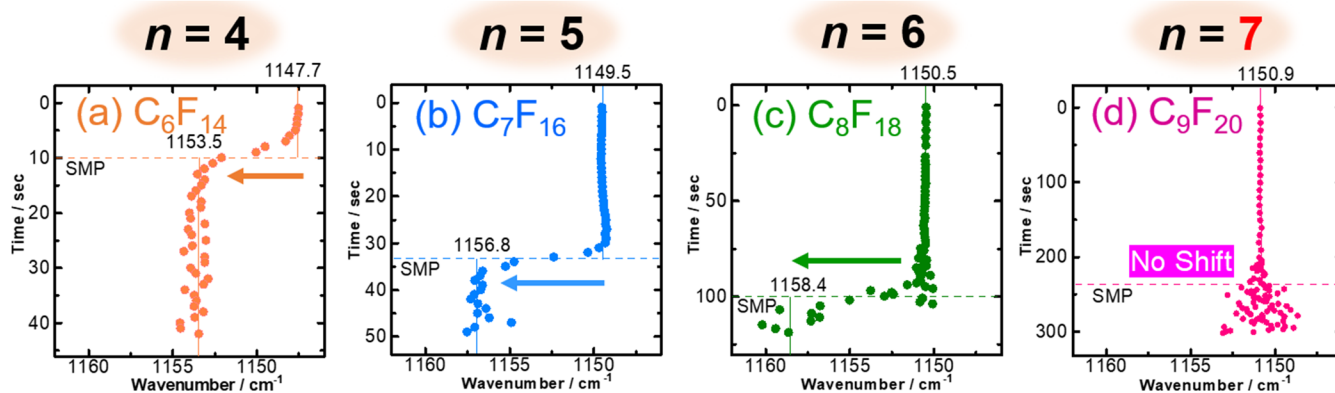


FIG. 6. Peak shift of $\nu_s(\text{CF}_2)$ with time. (a) C_6F_{14} ; (b) C_7F_{16} ; (c) C_8F_{18} ; (d) C_9F_{20} .

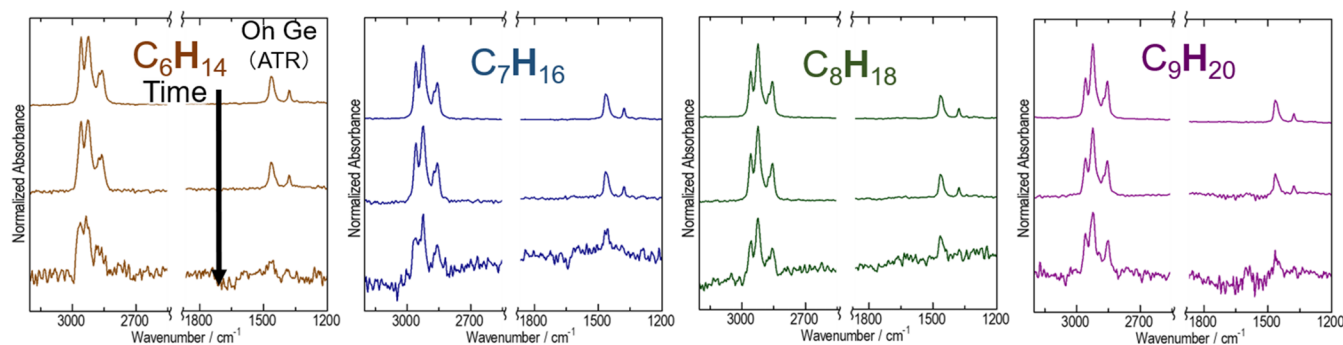


FIG. 7. IR ATR spectra of hydrocarbons corresponding to the R_f compounds in terms of the chain length.

due to $n = 7$ remain accounting for the no shift. This significant difference from the shorter compounds strongly supports the spontaneous molecular aggregation via the D–D interaction as expected by the SDA theory.

All the discussion made above is on a theoretical hypothesis that the D–D interaction is key to understand the surface modes and the SDA packing. To confirm this theoretical basis, the same experiments were repeated for hydrocarbons (normal alkanes) having the same length. Figure 7 presents normalized IR ATR spectra of liquid hydrocarbons ranging from C6 to C9. With time, only the spectral “intensity” decreases leaving the spectral shape unchanged, which is totally different from those of perfluoroalkanes (Fig. 2). This result simply implies that the significant change in shape found for perfluoroalkanes is truly induced by the large polarity on the molecule.

SUMMARY

Spectroscopic analysis of R_f compounds accompanies a significant change in spectral “shape” on thickness change of the sample, which makes the conventional analysis very difficult in the case of fluorocarbons. In the present study, through the thickness change of a simple R_f compound, the intrinsic difference from the

corresponding hydrocarbon is revealed by considering the surface modes related to Berreman’s phonon and particle polariton modes. After a theoretical comparison with the case of inorganic ionic crystals, useful selection rules for the analysis of a very thin film of an organic compound are obtained. With the use of the rules, the last moment of the evaporation of perfluoroalkanes is found to have a discontinuous film irrespective of the R_f length in the range of C6 through C9. In addition, on appearance of the surface-mode band, a significantly large shift of the $\nu_s(\text{CF}_2)$ band was also found simultaneously, which is comprehensively understood by the SDA theory. In other words, the SDA theory has paradoxically been confirmed in a spectroscopic manner.

Furthermore, the long-term matter of the band at 1234 cm^{-1} has been confirmed to be the bulk TO mode that is significantly shifted to the surface mode at 1255 cm^{-1} . When the sample thickness is not thin, the bulk TO mode dominates the spectra, whereas the surface mode that is similar to the bulk LO mode in shape becomes dominant for a very thin film. Since the anti-symmetric stretching vibration mode generally has an apparently stronger intensity than the symmetric one,¹⁴ the origin of the bulk TO mode should be attributed to the $\nu_a\text{CF}_2$ mode of a single R_f group, whereas the corresponding $\nu_s\text{CF}_2$ mode remains as a normal mode because of the relatively weak intensity. In this manner, the assignments of the two CF_2 stretching vibration bands have also been revealed at last.

ACKNOWLEDGMENTS

This work was financially supported by a Grant-in-Aid for Scientific Research (A) [Grant No. 15H02185 (T.H.)], Grant-in-Aid for Young Scientists (B) [Grant No. 17K14502 (T.S.)], and Grant-in-Aid for Early-Career Scientists [Grant No. 19K15602 (N.S.)] from the Japan Society for the Promotion of Science (JSPS), to which the authors' thanks are due.

DATA AVAILABILITY

The data that support the findings of this study are available within the article.

REFERENCES

- ¹T. Hasegawa, T. Shimoaka, N. Shioya, K. Morita, M. Sonoyama, T. Takagi, and T. Kanamori, *ChemPlusChem* **79**, 1421 (2014).
- ²T. Hasegawa, *Chem. Rec.* **17**, 903 (2017).
- ³T. Shimoaka, Y. Tanaka, N. Shioya, K. Morita, M. Sonoyama, H. Amii, T. Takagi, T. Kanamori, and T. Hasegawa, *J. Colloid Interface Sci.* **483**, 353 (2016).
- ⁴R. Kise, A. Fukumi, N. Shioya, T. Shimoaka, M. Sonoyama, H. Amii, T. Takagi, T. Kanamori, K. Eda, and T. Hasegawa, *Bull. Chem. Soc. Jpn.* **92**, 785 (2019).
- ⁵K. Ariga and L. K. Shrestha, *APL Mater.* **7**, 120903 (2019).
- ⁶V. P. Tolstoy, I. V. Chernyshova, and V. A. Skryshevsky, *Handbook of Infrared Spectroscopy of Ultrathin Films* (Wiley, Hoboken, NJ, 2003).
- ⁷T. Hasegawa, *Quantitative Infrared Spectroscopy for Understanding of a Condensed Matter* (Springer, Tokyo, 2017).
- ⁸T. Hasegawa, *Chem. Phys. Lett.* **627**, 64 (2015).
- ⁹F. London, *Trans. Faraday Soc.* **33**, 8 (1937).
- ¹⁰M. J. Hannon, F. J. Boerio, and J. L. Koenig, *J. Chem. Phys.* **50**, 2829 (1968).
- ¹¹T. Shimoaka, M. Sonoyama, H. Amii, T. Takagi, T. Kanamori, and T. Hasegawa, *J. Phys. Chem. A* **121**, 8425 (2017).
- ¹²T. Shimoaka, M. Sonoyama, H. Amii, T. Takagi, T. Kanamori, and T. Hasegawa, *J. Phys. Chem. A* **123**, 3985 (2019).
- ¹³N. Nagai, M. Okawara, and Y. Kijima, *Appl. Spectrosc.* **70**, 1278 (2015).
- ¹⁴N. Nagai, H. Okada, and T. Hasegawa, *AIP Adv.* **9**, 105203 (2019).
- ¹⁵C. Kittel, *Introduction to Solid State Physics*, 8th ed. (Wiley, Hoboken, NJ, 2005).
- ¹⁶V. M. Agranovich and D. L. Mills, *Surface Polaritons* (North-Holland Publishing Company, 1982).
- ¹⁷R. Ruppin and R. Englman, *Rep. Prog. Phys.* **33**, 149 (1970).
- ¹⁸D. W. Berreman, *Phys. Rev.* **130**, 2193 (1963).
- ¹⁹T. Hasegawa, T. Shimoaka, Y. Tanaka, N. Shioya, K. Morita, M. Sonoyama, H. Amii, T. Takagi, and T. Kanamori, *Chem. Lett.* **44**, 834 (2015).
- ²⁰T. Shimoaka, H. Ukai, K. Kurishima, K. Takei, N. Yamada, and T. Hasegawa, *J. Phys. Chem. C* **122**, 22018 (2018).
- ²¹G. J. Moody and J. D. R. Thomas, *Dipole Moments in Inorganic Chemistry* (Edward Arnold, London, 1971).
- ²²R. H. Lyddane, R. G. Sachs, and E. Teller, *Phys. Rev.* **59**, 673 (1941).
- ²³J. Shanker, G. G. Agrawal, and R. Pal Singh, *Philos. Mag. B* **39**, 405 (1979).
- ²⁴T. Hasegawa, S. Takeda, A. Kawaguchi, and J. Umemura, *Langmuir* **11**, 1236 (1995).
- ²⁵R. G. Greenler, *J. Chem. Phys.* **44**, 310 (1966).
- ²⁶K. L. Kliewer and R. Fuchs, *Phys. Rev.* **150**, 573 (1966).
- ²⁷K. L. Kliewer and R. Fuchs, *Phys. Rev.* **144**, 495 (1966).
- ²⁸H. Fröhlich, *Theory of Dielectrics* (Oxford at the Clarendon Press, 1949).
- ²⁹J. S. Plaskett and P. N. Schatz, *J. Chem. Phys.* **38**, 612 (1963).